Chapter 3

Nonclassical effects in quadratically coupled OMS

3.1 Introduction

Optomechanics is a promising candidate; the attention of the researcher has been drawn to it, recently. Different types of optomechanical architectures are reported in different experimental set up and theoretical studies such as macroscopic mirrors suspended in a cavity, micro-pillars suspended in a cavity, membrane placed inside a cavity, microtoroid, semiconductor microdisk resonator, microsphere resonator, nano-rod inside a cavity, cold atoms in a cavity, flying atom in a cavity etc [69, 71, 74, 128-131]. Here, we are interested to an OMS, where a membrane (dielectric) is placed inside two high-finesse, rigid and macroscopic mirrors [71]. In this system the coupling between mechanical membrane and e. m. degrees of freedom, is varied quadratically with membrane displacement. Generally, the coupling may vary with linear or square of the displacement. For example, OMS with photon induced tunnelling [132], single photon emission [133] are connected with linear coupling whereas system with strong dispersive coupling [71], ultra-cold atoms [134] and micro-disk resonators [135] have connection with quadratic coupling. Recently, in ref. [136] Brunelli et al studied the nonclassical states in OMS with both linear as well as quadratic coupling. There are advantages of quadratically coupled system over linearly coupled system as for QND measurements of photon and phonon [71], optical springs [137], photon transport [138], cooling and trapping of reflective mirror [139] and optical trapping of dielectric particles [140]. Motivated by the above possible utilities we have illustrated the OMS with quadratic coupling.

Nonclassical states are more interesting and these are also studied in quadratic OMS [141-144]. Nunnenkamp et al has described phonon cooling of mechanical oscillator and mechanical squeezing of quadratic OMS, where cavity is driven by two beams

[141]. Photon statistics, bipartite entanglement between optical and mechanical mode, squeezing and temporal evolution of Wigner function of mechanical oscillator is described in absence of driving and dissipation [142]. In ref. [143] Machado et al theoretically established superposition of states and squeezed state of the mechanical oscillator. The photon antibunching in weak-coupling regime is studied by Seok and Wright [144]. All these studies are made with lower order and in weak coupling regime.

In our study, we have investigated different nonclassical effects in moderate and strong coupling regime. We have also studied these nonclassical effects in higher order, where degree of nonclassicalities is expected to be enriched. We have analyzed the system in two ways: First, analytically solved the system Hamiltonian in absence of driving and dissipation (considering quantum system as closed). Second, to account loss factor and driving, we have made a numerical solution.

3.2 The Model Hamiltonian and its solution

The model system consists of a Fabry-Perot cavity and a dielectric membrane is placed inside at the middle of it [71], as depicted in figure 3.1. This type of configuration may be called as 'membrane-in-the-middle' configuration. The Hamiltonian of the system is written as

$$H = H_{sys} + H_{int} + H_{dri} \tag{3.1}$$

where, first part of it represents the Hamiltonian of the optical and mechanical mode, is described by $H_{sys} = \omega_c a^\dagger a + \omega_m b^\dagger b$. The resonance frequency for cavity field mode is represented by ω_c and ω_m represents the frequency of the mechanical motion. $a(a^\dagger)$ and $b(b^\dagger)$ are the lowering (raising) operator corresponds to optical mode and mechanical mode. Second part represents the interaction part of and expressed by

$H_{int} = ga^{\dagger}a(b^{\dagger} + b)^2$. g is the strength of coupling between the optical and mechanical mode. Last part corresponds to driving term $H_{dri} = iE(a^{\dagger}e^{-i\omega_d t} - ae^{i\omega_d t})$, where ω_d is the real driving strength with driving strength E.

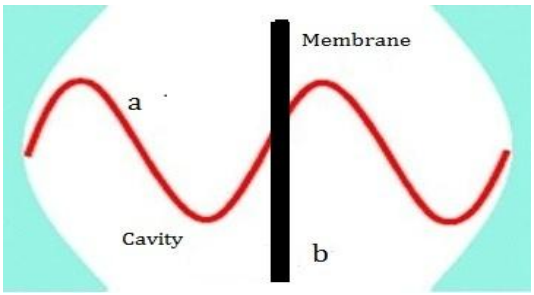

Figure 3.1: Schematic diagram of the model system with 'membrane-in-the-middle' configuration.

So, the Hamiltonian of the system takes the form

$$H = \omega_c a^{\dagger}a + \omega_m b^{\dagger}b + ga^{\dagger}a(b^{\dagger} + b)^2 + iE(a^{\dagger}e^{-i\omega_d t} - ae^{i\omega_d t}) \qquad (3.2)$$

To consider this system Hamiltonian we have made following assumptions: First, theoretical study [145] and experimental evidence [146] have shown that in OMS, the environmental effects are negligible. Second, at strong coupling regime the cavity loss rate are much smaller than optomechanical coupling strength. Third, we have analyzed the system Hamiltonian without driving term as some previous theoretical studies [147, 148] have been done in absence of driving. So, the system Hamiltonian of equation (3.2) becomes

$$H = \omega_c a^{\dagger}a + \omega_m b^{\dagger}b + ga^{\dagger}a(b^{\dagger} + b)^2 \qquad (3.3)$$

Using Heisenberg EOM, we obtain the differential equations correspond to cavity and mechanical modes are as follows:

$$\frac{da(t)}{dt} = -i[\omega_c a(t) + ga(t)\{b^{\dagger 2}(t) + b^2(t) + 2b^{\dagger}(t)b(t) + 1\}]$$

$$\frac{db(t)}{dt} = -i[\omega_m b(t) + 2ga^{\dagger}(t)a(t)\{b^{\dagger}(t) + b(t)\}] \qquad (3.4)$$

Using Taylor series expansion of a field operator we assume n-th order solution of the field modes are

$$a^n(t) = A_1^n a^n(0) + nA_1^{n-1}\{A_2 a^n(0)b^{\dagger 2}(0) + A_3 a^n(0)b^2(0) + A_4 a^n(0)b^\dagger(0)b(0) + A_5 a^n(0)\}$$

$$b^n(t) = B_1^n b^n(0) + nB_1^{n-1}\{B_2 a^\dagger(0)a(0)b^n(0) + B_3 a^\dagger(0)a(0)b^\dagger(0)b^{n-1}(0)\}$$
$$+\left\{\frac{n(n-1)}{2}\right\} B_1^{n-1}\, a^\dagger(0)a(0)b^n(0) \qquad (3.5)$$

where the parameters $A_i's$ and $B_i's$ are function of time and found out from boundary conditions $A_1(0) = B_1(0) = 1$ and $A_i(0) = B_i(0) = 0$ $[i = 2, \dots, 5]$.

The time dependent coefficients $A_i(t)$and $B_i(t)$ are given by (corresponding differential equations are in appendix A)

$$A_1(t) = \exp(-i\omega_c t)\ ;\ A_2(t) = \frac{\lambda}{2\omega_m} A_1(t)\{1 - \exp(2i\omega_m t)\}\ ;$$

$$A_3(t) = -A_2^*(t)A_1^2(t)\ ;\ A_4(t) = -2igtA_1(t)\ ;\ A_5(t) = A_4(t)/2\ ;$$

$$B_1(t) = \exp(-i\omega_m t)\ ;\ B_2(t) = -2igtB_1(t)\ ;\ B_3(t) = -\frac{2ig}{\omega_m}\sin\omega_m t. \quad (3.6)$$

The validity of the solution is checked by using equal time commutation relation

$$[a(t),\ a^\dagger(t)] = [b(t),\ b^\dagger(t)] = 1.$$

Using solutions of equation (3.5) and putting $n = 1$, we have obtained the number operators for the field mode a and b, and are given by

$$N_a = a^\dagger(t)a(t) =$$

$$a^\dagger(0)a(0)A_1^*A_1 + [a^\dagger(0)a(0)b^2(0)A_2^*A_1 + a^\dagger(0)a(0)b^{\dagger 2}(0)A_3^*A_1 +$$

$$a^\dagger(0)a(0)b^\dagger(0)b(0)A_4^*A_1 + a^\dagger(0)a(0)A_5^*A_1 + h.c.]$$

$$N_b = b^\dagger(t)b(t) =$$

$$b^\dagger(0)b(0)B_1^*B_1 + [a^\dagger(0)a(0)b^\dagger(0)b(0)B_2^*B_1 + a^\dagger(0)a(0)b^2(0)B_3^*B_1 + h.c.] \quad (3.7)$$

Here h.c. indicates Hermitian conjugate. In order to calculate different nonclassical correlation factors we consider the initial state is product of two coherent states and is expressed by $|\mathcal{U}\rangle = |\alpha\rangle \otimes |\beta\rangle$ where $|\alpha\rangle$and $|\beta\rangle$ are the eigenkets of field modes a and b respectively. If the operator $a(t)$ operates on the composite state $|\mathcal{U}\rangle$ it gives the complex eigenvalue α i.e. $a(t)|\mathcal{U}\rangle = \alpha|\mathcal{U}\rangle$ where $|\alpha|^2$ represents the photon number of the optical field mode a. Similarly, we obtain phonon number $|\beta|^2$ for mechanical mode b.

In next sections, different nonclassical effects are discussed both in lower as well as higher order by using corresponding nonclassical criteria. The systems parameters are used here, based on different experimental optomechanical setup. The mechanical frequency of the membrane varies from several kHz to MHz [71, 74, 79]. The strength of optomechanical coupling can be order of kHz [79, 149] and near field study shows that its value is order of few MHz [150].

3.3 Quadrature Squeezing

In present section, we have discussed the possibility of different types of squeezing such as single mode squeezing, compound mode squeezing, spin squeezing, difference and sum squeezing and variations of different squeezing parameters with system parameters are also reported.

3.3.1 Single mode squeezing

Here we have analyzed the single mode squeezing for both the field modes via lower as well as higher order variations. Using equation (2.5) and (3.5), the variance of the field quadratures are obtained as

$$\binom{(\Delta X_a)^2}{(\Delta Y_a)^2} = \frac{1}{4}[1 + (A_1^* A_2 \beta^{*2} + A_1^* A_3 \beta^2 + A_1^* A_4 |\beta|^2 + A_1^* A_5 + c.c.)] \quad (3.8)$$

$$\binom{(\Delta X_b)^2}{(\Delta Y_b)^2} = \frac{1}{4}[1 + (A_2^* A_1 |\alpha|^2 + c.c.) \pm (A_3 A_1 |\alpha|^2 + c.c.)] \qquad (3.9)$$

Here c.c. indicates complex conjugates. From equation (3.8) it is clear that lower order single mode squeezing is not possible for optical field mode as the variance of the field quadratures are always greater than zero point fluctuations.

Temporal variation of the field quadratures (equation 3.9) are plotted in fig. 3.2 (a, b). From the variations it is clear that there is signature of mechanical squeezing. The degree of squeezing increases with coupling strength. From the equation (3.9), it is clear that the degree of squeezing is independent of the phase of the input state.

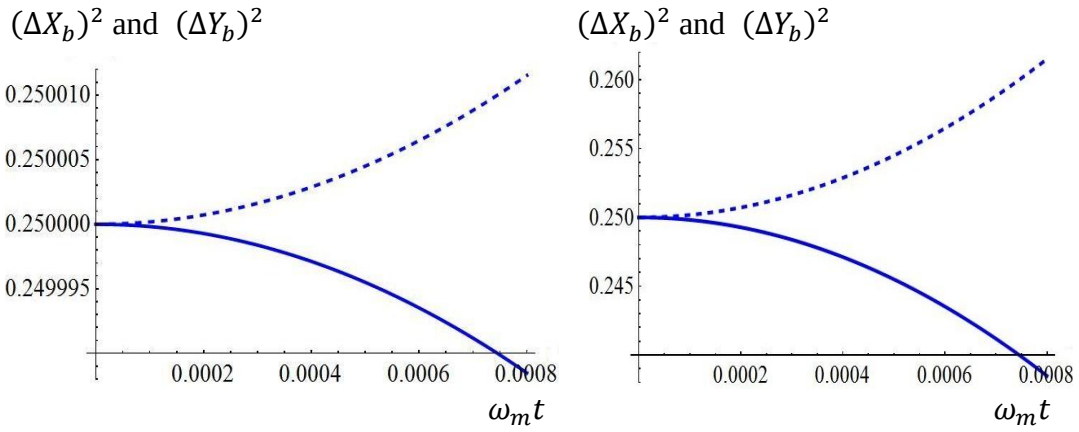

(a) (b)

Figure 3.2: Variation of the field quadrature variances $(\Delta X_b)^2$ (solid line) and $(\Delta Y_b)^2$ (dashed line) with rescaled time $\omega_m t$. The parameters are $|\alpha| = 3$, $|\beta| = 2$ (a) $g/\omega_m = 2$, $g = 1.2$ MHz (b) $g/\omega_m = 2\,000$, $g = 1.2$ GHz.

Using equation (2.11) and (3.5), we obtain the higher order squeezing factors as follows:

$$\binom{S_{1a}(n)}{S_{2a}(n)} = 0 \qquad (3.10)$$

$$\binom{S_{1b}(n)}{S_{2b}(n)} = \pm\frac{n^2}{4} |\alpha|^2 (B_3 B_1^{2n-1} \beta^{2n-2} + c.c.) \qquad (3.11)$$

From equation (3.10) it is clear that higher order squeezing is not possible for optical mode. But for mechanical mode there is signature of higher order squeezing. To study the variation of the squeezing factors we plot right side of the equation (3.11) in figure 3.3. Figure (a) displays the variation for $n = 2$ i.e. amplitude squared and figure (b) for $n = 3$ i.e. amplitude cube squeezing. From these it is clear that any one squeezing parameter is always less than zero i.e. squeezed due to expense of other. The degree of squeezing increases with order number. This is due to presence of the term $n^2\beta^{2n-2}$ in the expression, which plays the role of amplification factor. Interestingly, it is also observed that time period of oscillations is shortened with order number. As order number increases the energy exchange decreases and hence time period of oscillations decreases. The degree of squeezing can also be tuned via weight factor of the initial state. For a given order number the squeezing factor also increases with optomechanical coupling strength. This can be explained as due to the presence of the term $B_3(t)$ in the expression of equation (3.11).

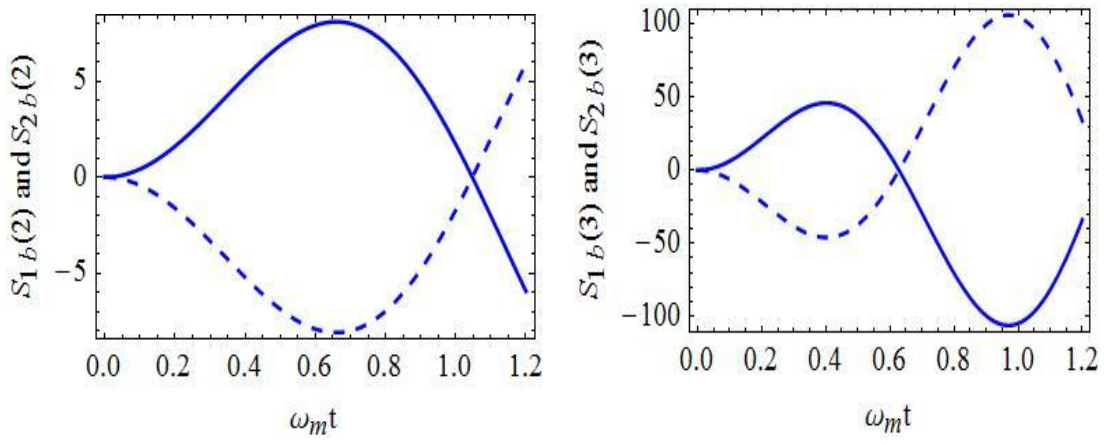

(a) (b)

Figure 3.3: Variation of squeezing factors $S_{1b}(n)$ (solid line) and $S_{2b}(n)$ (dashed line) with $\omega_m t$ for mechanical mode with $|\alpha| = 3$, $|\beta| = 2$, $g = 2\pi \times 10$ KHz and $g/\omega_m = 0.1$ (a) $n = 2$ (b) $n = 3$.

Figure 3.4 depicts the variation of the higher order squeezing factors of the mechanical mode (equation 3.11) with time. This shows collapse-revival phenomena, the occurrence of it is explained as follows: The squeezing factors $S_{ib}(n)$ contain two periodic functions of the form $f(\omega_m t)$ and $f(n\omega_m t)$. For a certain value of ω_m , the period of energy exchange between the modes lowered, many oscillations occurred up-to interaction time $\omega_m t = p\pi$, p is a positive integer. When the field is trapped by the nonlinearity of the membrane, $S_{ib}(n)$ collapsed. As phononic interaction proceeds the patterns repeat periodically. The number of revival patterns increases with order number, due to the period of revival phenomena is steered by the factor $t = \frac{2\pi}{(2n-1)\omega_m}$. Mathematically, the term $B_3(t)$ plays the key role for revival and envelope function $B_1(t)$ gives the main contribution to the collapse.

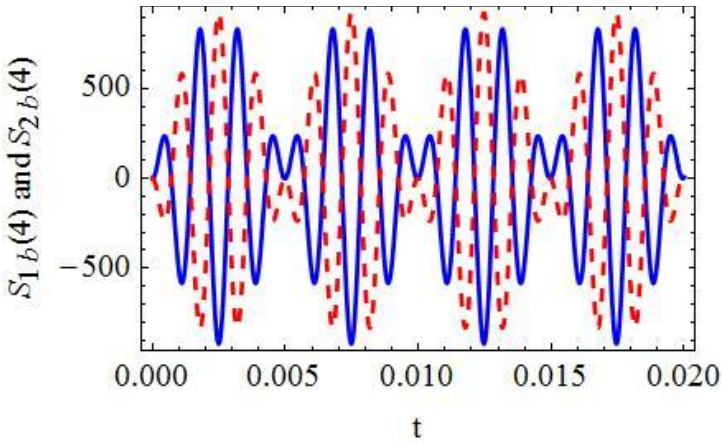

Figure 3.4: Plot of $S_{1b}(4)$ (blue solid line) and $S_{2b}(4)$ (red dashed line) with t(ms) for b mode with n=4, $|\alpha| = 3$, $|\beta| = 2$, $g = 2\pi \times 10$ KHz and $g/\omega_m = 0.1$.

3.3.2 Compound mode squeezing

Using equation (2.7) and (3.5) we obtain

$$\begin{pmatrix}(\Delta X_{ab})^2\\(\Delta Y_{ab})^2\end{pmatrix} = \frac{1}{2}\left[\begin{pmatrix}(\Delta X_a)^2\\(\Delta Y_a)^2\end{pmatrix} + \begin{pmatrix}(\Delta X_b)^2\\(\Delta Y_b)^2\end{pmatrix}\right]$$

$$+\frac{1}{8}\{(2B_1^*A_3 + B_3^*A_1)\alpha\beta + (2B_1^*A_4 + B_2^*A_1)\alpha\beta^* + c.c.\}$$

$$\pm\frac{1}{8}[\{(A_1B_2 + A_4B_1)\alpha\beta + (A_1B_3 + 2A_2B_1)\alpha\beta^*\} + c.c.] \quad (3.12)$$

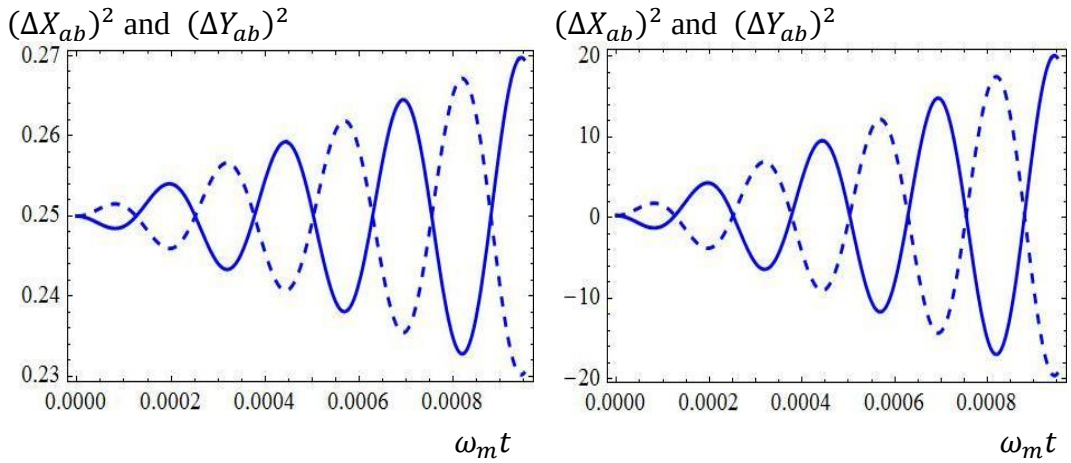

Figure 3.5: Variation of compound mode field quadrature $(\Delta X_{ab})^2$ (solid line) and $(\Delta Y_{ab})^2$ (dashed line) with rescaled time $\omega_m t$. The parameters are $|\alpha| = 3$, $|\beta| = 2$ (a) $g/\omega_m = 2$, $g = 1.2$ MHz (b) $g/\omega_m = 2\,000$, $g = 1.2$ GHz.

The right side of equation (3.12) is plotted in figure (3.5) for different coupling strength. From the variation it is cleared that there is a signature of compound mode squeezing and degree of squeezing is increased with coupling strength. Any one of the field quadrature is always squeezed due to cost of other. It is also shown that degree of compound squeezing is more as compared to single mode mechanical squeezing. The monotonous increase of envelop of the field quadrature is due to truncation of the calculations of the interaction term.

3.3.3 Spin squeezing

Using solutions of equation (3.5) and different spin squeezing operator (equation 2.16), we obtain variance of S_x, S_y and average value of S_z as follows:

$$\langle(\Delta S_x)^2\rangle = \frac{1}{4}[|A_1|^2|B_1|^2(|\alpha|^2+|\beta|^2) + \{A_1^2B_3^*B_1^*\alpha^*\alpha^3 + 2(A_2^*A_1 + B_3^*B_1)|\alpha|^2\beta^2 + c.c.\}]$$

$$\left\langle\left(\Delta S_y\right)^2\right\rangle = \frac{1}{4}[|A_1|^2|B_1|^2(|\alpha|^2+|\beta|^2) + \{2(A_2^*A_1 + B_3^*B_1)|\alpha|^2\beta^2 - A_1^2B_3^*B_1^*\alpha^*\alpha^3 + c.c.\}]$$

$$\langle S_z\rangle = \tfrac{1}{2}\{|A_1|^2|\alpha|^2 - |B_1|^2|\beta|^2 - (B_3^*B_1|\alpha|^2\beta^2 + c.c.\} \quad (3.13)$$

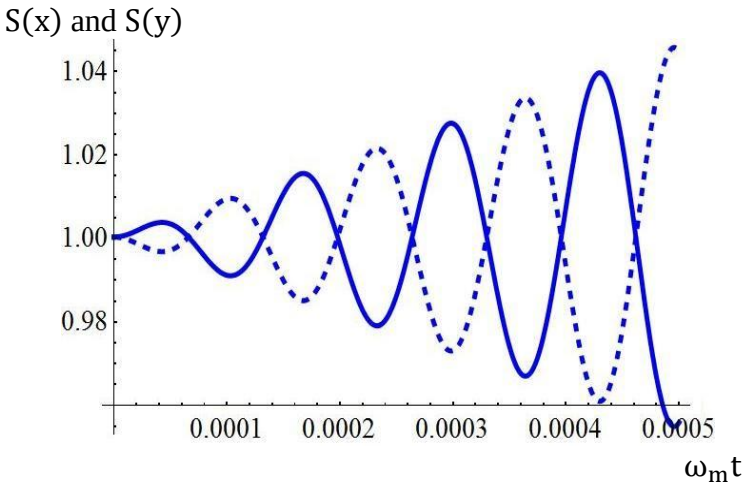

Figure 3.6: Plot of spin squeezing factors S(x) (solid line) and S(y) (dashed line) with rescaled time $\omega_m t$. The parameters are $|\alpha| = 3, |\beta| = 2$, $g = 2\pi \times 0.4$ KHz and $g/\omega_m = 0.004$.

Using above and equation (2.17) we have plotted the temporal variation of the squeezing factors $S(x)$ and $S(y)$ in figure (3.6). It is evident that any one squeezing factor is always less than one. So, any one spin component S_x or S_y is always squeezed due to energy exchange in between one another. The degree of squeezing can be tuned via coupling strength.

3.3.4 Sum and Difference squeezing

In this portion we have analyzed the possibility of sum and difference squeezing in the present system. To study the variation of squeezing factors, we consider optical mode is initially coherent and mechanical mode is in vacuum state. So, the initial state is $|\mathcal{U}\rangle = |\alpha\rangle \otimes |0\rangle$. Using equation (2.9) and solutions of equation (3.5) and (3.7), we find the sum squeezing factors as follows:

$$\begin{pmatrix} S_{1_{ab}} \\ S_{2_{ab}} \end{pmatrix} = \pm\frac{1}{4}[A_1^2 B_3 B_1 \alpha^2(2 + |\alpha|^2) + c.c.] \tag{3.14}$$

The right side of the above expression is not simple, if we simplify then it is evident that it's function of sum of the frequency for mechanical and optical mode. So, sum of two frequencies can be generated via this study.

Again, using equation (2.10) and solutions of equation (3.5) and (3.7), difference squeezing factors are obtained as follows:

$$\begin{pmatrix} Q_{1_{ab}} \\ Q_{2_{ab}} \end{pmatrix} = \pm\frac{1}{4}[A_1^2 B_1^* B_3^* \alpha^* \alpha^3 + c.c.] \tag{3.15}$$

To calculate the difference squeezing factors we have used $N_a > N_b$ i.e. Hillery's condition of difference squeezing [98]. Analyzing the above equation (3.15) it is clear that output of the difference squeezed state is a function of difference between the cavity and mechanical mode frequencies.

To study the variation of the squeezing factors, we plot the equation (3.14 and 3.15) as a function of normalized time in figure 3.7(a) and (b), respectively. Both the plots show that the envelope of the squeezing factors monotonically increase, explanation of this is same as for compound mode squeezing (sub-section 3.3.2). The degree of squeezing for both cases may be tuned by coupling strength and phase of the input state. But for same interaction parameters the degree of difference squeezing is almost 50% of sum

squeezing. The degree of difference squeezing is reduced due to dephasing between optical and mechanical mode.

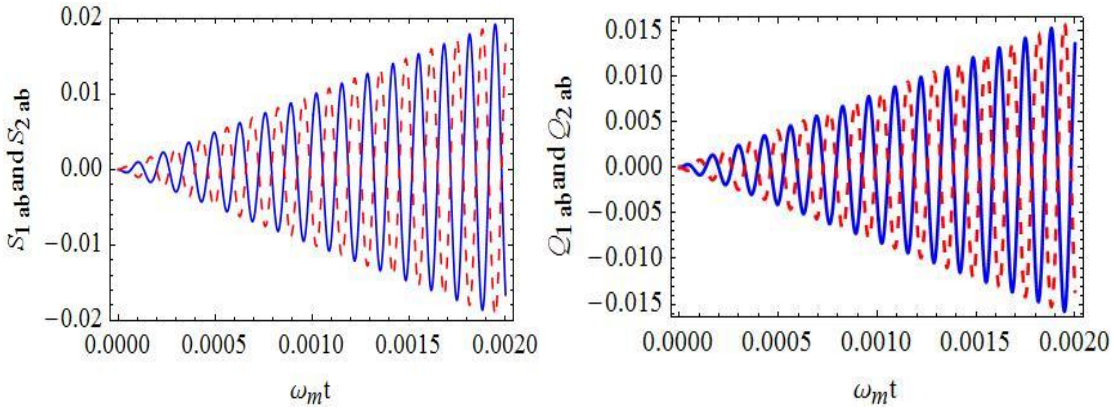

(a) (b)

Figure 3.7: Plot of (a) sum squeezing parameters $S_{1_{ab}}$ (blue solid line) and $S_{2_{ab}}$ (red dashed line) and (b) difference squeezing parameters $Q_{1_{ab}}$ (blue solid line) and $Q_{2_{ab}}$ (red dashed line) with $\omega_m t$ for $|\alpha| = 3$, $g = 2\pi \times 10$ KHz and $g/\omega_m = 0.1$.

3.4 Quantum Statistics

In this section, we have discussed the particle statistics for quadratically coupled OMS. The particle statistics are studied for both the single field mode and their inter-mode in following two sub-sections.

3.4.1 Single mode statistics

Using equation (2.22) and solutions (equation 3.5 and 3.7) we obtain the following expressions of antibunching factors for cavity field mode and mechanical mode.

$$A_a(n) = 0 \tag{3.16}$$

$$A_b(n) = \frac{n(n+1)}{2}\left(B_3^* B_1 \beta^{*(n-1)} \beta^{n+1} + c.c.\right) \tag{3.17}$$

From the result of equation (3.16) it is clear that antibunching factor for optical mode is zero. So, the photon mode shows Poissonian statistics i.e. optical mode is coherent. By

simplifying the equation (3.17), it is obtained that the result is always positive for a set of system parameters. So, phonon mode shows super-Poissonian nature i.e. phonon bunching. From this study, it is concluded that single mode antibunching is not possible for the dynamics of the present system.

3.4.2 Intermodal statistics

Using equation (2.24) and solutions (equation 3.5 and 3.7) we obtain the expression of $A_{ab}(n)$ as follows:

$$A_{ab}(n) = (|A_1|^{2n}|\alpha|^{2n} - |B_1|^{2n}|\beta|^{2n})(|\alpha|^2 - |\beta|^2) + B_3^* B_1 |\alpha|^2 \beta^{*(n-1)} \beta^{n+1} \left\{(n+1)\beta^* - n|\alpha|^2 + \frac{n(n-3)}{2}\right\} - B_3^* B_1 \left\{|\alpha|^{2n}\beta^2(n+|\alpha|^2) + \frac{n(n-1)}{2}|\alpha|^2\beta^{*n-2}\beta^n(2+|\alpha|^2)\right\} + c.c. \quad (3.18)$$

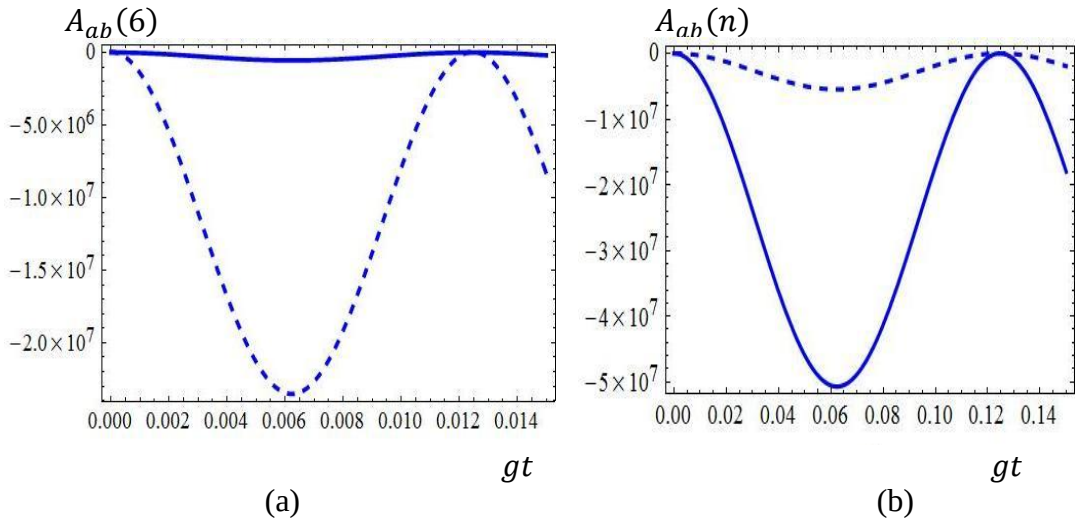

(a) (b)

Figure 3.8: Variation of compound mode antibunching factor $A_{ab}(n)$ with rescaled time gt with (a) n = 6, |β| = 2, $g = 2\pi \times 0.4$ KHz, $g/\omega_m = 0.004$, |α| = 3 (solid curve) and |α| = 4 (dashed curve) (b) |α| = 3 , |β| = 2, $g = 2\pi \times 0.4$ KHz, $g/\omega_m = 0.004$, n = 7 (solid curve) and n = 6 (dashed curve).

The temporal variation of equation (3.18) is depicted in figure 3.8 (a, b) for different weight factor of input, coupling strength and order number. The plots shown that the

value of $A_{ab}(n)$ is negative i.e. the statistics is super-Poissonian. So, there is a signature of intermodal antibunching. Figure (a) shows the variation of $A_{ab}(n)$ for order number $n = 6$ with cavity photon number $|\alpha|^2 = 9$ and $|\alpha|^2 = 16$. Thus the degree of antibunching depends on weight of the input state. Figure (b) displays the variation of $A_{ab}(n)$ for order number $n = 6$ and $n = 7$. From this variation it is clear that degree of intermodal antibunching is significantly increased with order number. From the analysis, it is also concluded that degree of squeezing can also be tuned by coupling strength.

3.5 Entanglement

Here, we have discussed the existence of another nonclassical properties called as entanglement in present system. We have studied the effect both in lower order via Duan et al criteria and Hillery-Zubairy criteria and higher order via Hillery-Zubairy criteria.

3.5.1 Lower order Entanglement

We first examine the possibility of lower order entanglement via Duan et al criteria (equation 2.26) and solutions of equation (3.5). We find the following analytical expression

$$(\Delta u)^2 + (\Delta v)^2 - 2 = [(A_1^* A_2 \beta^{*2} + A_1^* A_3 \beta^2 + A_1^* A_4 |\beta|^2 + A_1^* A_5 + B_2^* B_1 |\alpha|^2 + 2B_1^* A_3 \alpha\beta + B_3^* A_1 \alpha\beta + B_1^* A_4 \alpha\beta^* + B_3^* A_1 \alpha\beta^*) + c.c.] \quad (3.19)$$

The equation (3.19) is plotted in figure (3.9) as a function of time for different coupling strength. It is clear that the value of $(\Delta u)^2 + (\Delta v)^2 - 2$ is negative with a periodic nature and its negativity is increases with coupling strength. Interestingly, the parameter $(\Delta u)^2 + (\Delta v)^2 - 2$ oscillates between non-classical to classical regions. The degree of nonclassicality depends on weight factor and phase of the input state.

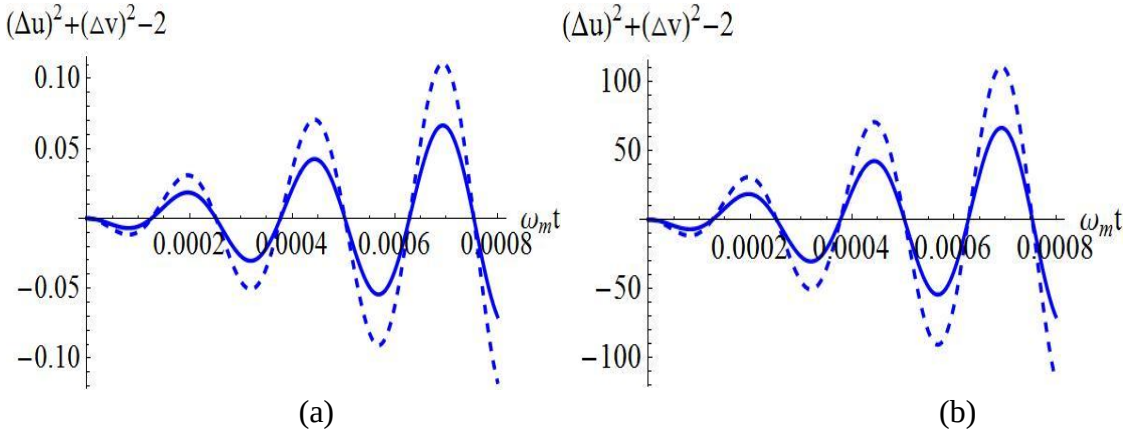

Figure 3.9: Variation of $(\Delta u)^2 + (\Delta v)^2 - 2$ with rescaled time $\omega_m t$ for $|\alpha| = 3$ (solid curve) and $|\alpha| = 5$ (dashed curve), $|\beta| = 2$ (a) $g/\omega_m = 2$, $g = 1.2$ MHz (b) $g/\omega_m = 2\,000$, $g = 1.2$ GHz.

Using Hillery-Zubairy criteria (equation 2.28) and solutions of equation (3.5) and (3.7), we obtain

$$E_{ab} = -[|\alpha|^2(B_1^* B_2|\beta|^2 + B_1^* B_3 \beta^{*2}) + c.c.] \tag{3.20}$$

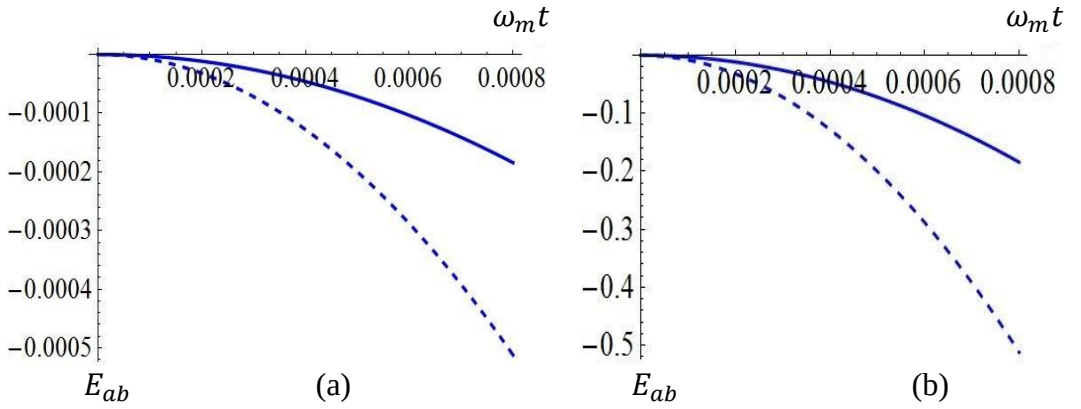

Figure 3.10: Variation of E_{ab} with rescaled time $\omega_m t$ for $|\alpha| = 3$ (solid curve) and $|\alpha| = 5$ (dashed curve), $|\beta| = 2$ (a) $g/\omega_m = 2$, $g = 1.2$ MHz (b) $g/\omega_m = 2\,000$, $g = 1.2$ GHz.

Figure (3.10) display the variation of E_{ab} as a function of time for different coupling strength. The negativity of the entanglement parameter E_{ab} shows the existence of intermodal entanglement in present system. Interestingly, the optical mode and

mechanical mode are initially separable but these are entangled via radiation pressure interaction.

3.5.2 Higher order Entanglement

To analyze higher order entanglement in quadratically coupled OMS, we have used Hillery-Zubairy criteria (equation 2.30 and 2.31) and solutions of equation 3.5 and 3.7, to obtain the analytical expression of $E_{ab}^{m,n}$ and $E_{ab}^{\prime m,n}$. These are as follows:

$$E_{ab}^{m,n} = [mn\{2(A_2^* A_1 \beta^{*(n-1)}\beta^{(n-1)} + c.c.) + (n-1)(A_2^* A_1 \beta^{*(n-2)}\beta^{n} + c.c.)\}$$

$$+ \frac{n(n-1)(m-1)}{2}(B_3^* B_1 \beta^{*(n-2)}\beta^{n} + c.c.)] \mid \alpha \mid^{2m} \quad (3.21)$$

$$E_{ab}^{\prime m,n} = -mn[(B_1^* B_3 \beta^{*2} + c.c) \mid \beta \mid^{2(n-1)}$$

$$+ \frac{(n-1)}{2}(B_1^* B_3 \beta^{*n}\beta^{n-2} + c.c.)] \mid \alpha \mid^{2m} \quad (3.22)$$

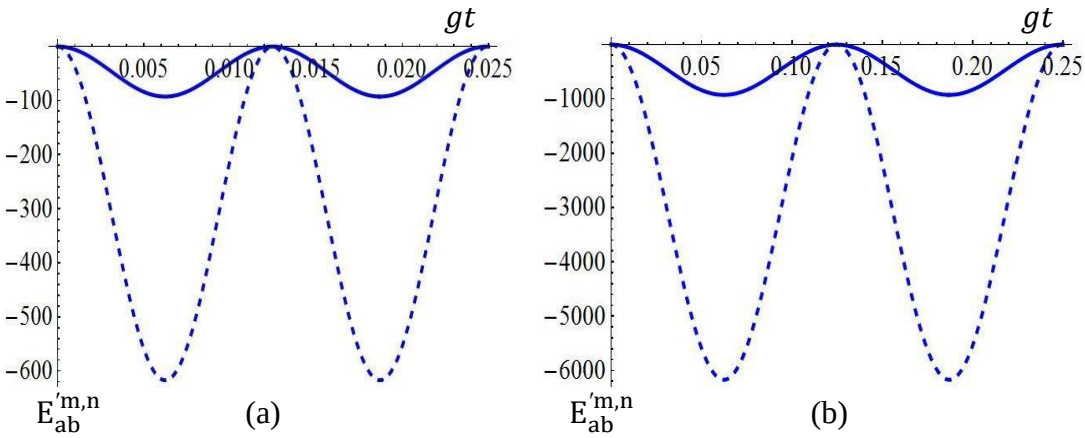

Figure 3.11: Variation of $E_{ab}^{\prime m,n}$ with rescaled time gt for $|\alpha| = 3, |\beta| = 2$, m = n = 2 (solid curve) and m = 2, n = 3 (dashed curve) (a) $g = 2\pi \times 0.4$ KHz, $g/\omega_m = 0.004$ (b) $g = 2\pi \times 4$ KHz, $g/\omega_m = 0.04$.

After simplification the expression $E_{ab}^{m,n}$ shows positive values for a set of parameters. But $E_{ab}^{\prime m,n}$ is always negative i.e. higher-order bipartite entangled state exists for present system. As these criteria are sufficient to characterize non-separable state but not

necessary. The right side of equation (3.22) is not so simple; we plot it as function of time in figure (3.11), for different order number. The negativity of entanglement parameter increases with coupling strength and order number. If we put $n = 1$ in equation (3.22) it reduces to equation (3.20) i.e. lower order entanglement. As order grow the degree of entanglement increases. This is due to the presence of the term $mn \mid \alpha \mid^{2m}$ in the expression, which acts as magnification factor. The graphical representation shows that non-separable state is in a periodic repetition. The periodicity of the entangled parameter is independent of the order number i.e. periodicity is same for all order.

3.6 Numerical Solution

In this section, we have analyzed the effect of optical loss, mechanical damping and driving term over nonclassical states viz. squeezing and entanglement. To account these we have taken master equation approach. To solve numerically we have required to RWA for the Hamiltonian of equation (3.2).

Under RWA the equation (3.2) takes the form

$$H_r = \Delta_a a^\dagger a + \omega_m b^\dagger b + g a^\dagger a (b^\dagger + b)^2 + E(a^\dagger + a) \tag{3.23}$$

Where $\Delta_a = \omega_c - \omega_d$ is the frequency detuning between the cavity and driving field.

The Lindblad's master equation for the system is given by

$$\begin{aligned} \dot{\rho} = -i[H_r, \rho] &+ \frac{k_0}{2}(2a\rho\, a^\dagger - a^\dagger a\rho - \rho\, a^\dagger a) \\ &+ \frac{\gamma}{2}(n_{th}+1)(2b\rho b^\dagger - b^\dagger b\rho - \rho\, b^\dagger b) \\ &+ \frac{\gamma}{2} n_{th}(2b^\dagger \rho b - bb^\dagger \rho - \rho\, bb^\dagger) \end{aligned} \tag{3.24}$$

k_0 and γ represent the decay rate and mechanical damping corresponds to the optical mode and mechanical mode, respectively and n_{th} is average thermal phonon numbers at temperature T, given by the formula $n_{th} = 1/\left\{\exp\left(\frac{\hbar\omega_m}{kT}\right) - 1\right\}$. Here, we have assumed average thermal cavity photon number is zero. The equation (3.24) is solved numerically using Fock state $n_a \otimes n_b$ as basis, where n_a and n_b indicate the photon and phonon numbers for the field modes a and b, respectively.

Using equation (2.5) and (2.7), we have plotted the variances of the field quadratures for mechanical and compound mode as a function of cavity detuning in figure 3.12(a) and (b). From these it is clear that both mechanical squeezing and compound mode squeezing. The degree of both the squeezing increases with the coupling strength. The degree of squeezing can also be controlled by driving strength.

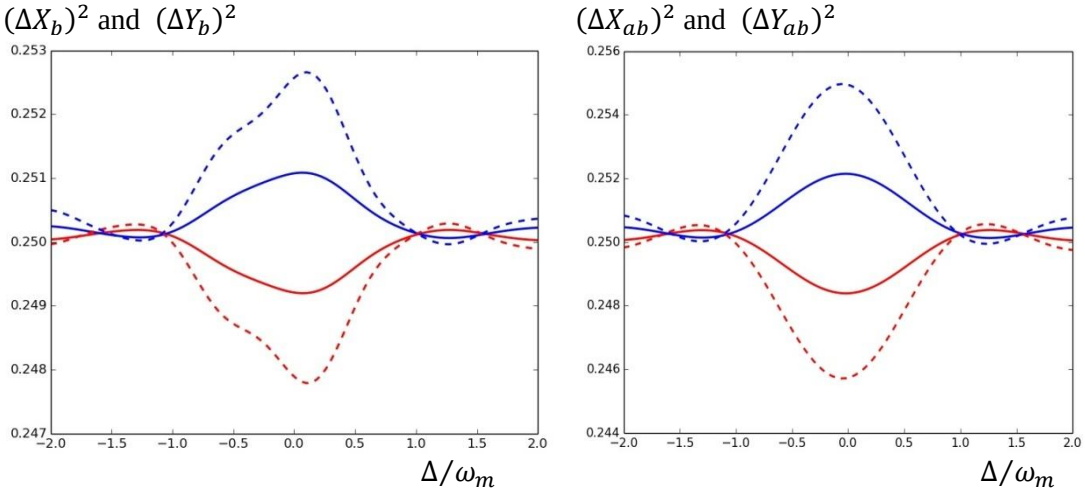

Figure 3.12: Plot of the variance of the field quadratures with normalised cavity detuning. (a) $(\Delta X_b)^2$ (solid blue line) and $(\Delta Y_b)^2$ (solid red line) for $g/\omega_m = 0.02$; $(\Delta X_b)^2$ (dashed blue line) and $(\Delta Y_b)^2$ (dashed red line) for $g/\omega_m = 0.05$ (b) $(\Delta X_{ab})^2$ (solid blue line) and $(\Delta Y_{ab})^2$ (solid red line) for $g/\omega_m = 0.02$; $(\Delta X_{ab})^2$ (dashed blue line) and $(\Delta Y_{ab})^2$ (dashed red line) for $g/\omega_m = 0.05$. The other parameters are $k_o/\omega_m = 0.1$, $\gamma/\omega_m = 10^{-7}$, $E/\omega_m = 0.1$, $T = 100mK$ and $n_{th} = 1000$.

Figure 3.13 depict the variation of entanglement parameter $(\Delta u)^2 + (\Delta v)^2 - 2$ as a function of cavity detuning for different coupling strength and it shows that degree of entanglement is changed slightly as coupling strength increases.

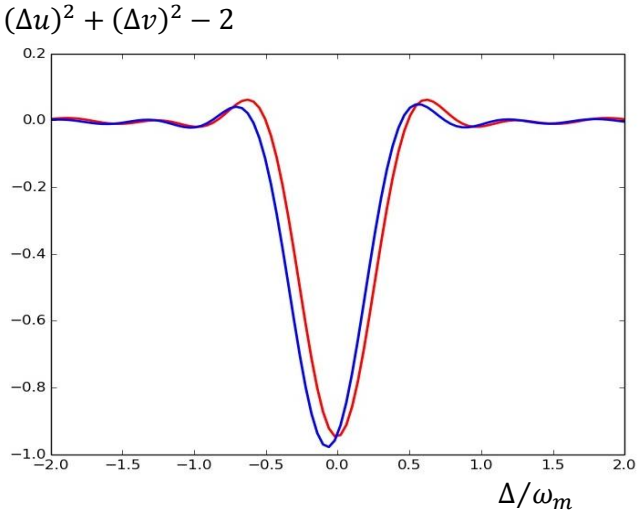

Figure 3.13: Variation of $(\Delta u)^2 + (\Delta v)^2 - 2$ with normalised cavity detuning for $g/\omega_m = 0.005$ (red line); $g/\omega_m = 0.08$ (blue line). The other parameters are $k_o/\omega_m = 0.1$, $\gamma/\omega_m = 10^{-7}$, $E/\omega_m = 0.1$, $T = 100mK$ and $n_{th} = 1000$.

3.7 Summary

In summary, we report lower and higher-order nonclassical effects in quadratically coupled OMS using a set of moment based criteria for single and compound mode squeezing, super-Poissonian statistics, intermodal entanglement. We have illustrated higher-order single mode squeezing, sum squeezing, difference squeezing, higher order particle statistics, higher order entanglement in the present system. None of these nonclassical effects were turned up by previous studies.

In the present work, the fluctuation of nonclassical effects with system parameters, such as optomechanical coupling strength, weight factor and phase of the input state and order number, are also reported, and it is observed that the degree of nonclassical effects can be tuned by system parameters.

The system Hamiltonian is solved analytically by using Heisenberg EOM for different field modes at moderate and strong coupling regime. Each EOM is solved by short time dynamics with Taylor series expansion of an operator. For strong coupling regime, the effects of loss factor and environmental effects are negligible. The coupling strength is varied in wide range of values, several kHz to GHz.

In this study, it is observed that cavity field mode is not squeezed but mechanical mode is squeezed for both lower and higher order. Higher order study shows that degree of squeezing increases with order. Interestingly, the time period of fluctuations of squeezing factor decreases as order grows. Again, mechanical squeezing factors also show revival-collapse phenomena, due to nonlinearity of the dielectric membrane. As order grow number of revival pattern increases. Although, there is no signature of single cavity field squeezing but compound mode squeezing between cavity field mode and mechanical mode is observed. The analysis of sum and difference squeezing show that these are useful for generation of sum and difference frequency of the cavity and mechanical mode. Difference and sum squeezing are class of higher order squeezing (second order). From the temporal variation of single mode 2^{nd} order mechanical squeezing, sum squeezing and difference squeezing, it is observed that degree of squeezing is optimum for sum squeezing. So, to extract information, sum squeezing plays best role in present system. Temporal evolution of spin squeezed state is shown that it is possible either in S_x or in S_y direction; which may be useful for noise reduction in optical signal.

From the analysis of the particle statistics of photon and phonon mode it is clear that there is no signature of single mode sub-Poissonian statistics i.e. antibunching in the present system. Photon statistics is Poissonian whereas phonon statistics is super-

Poissonian in nature. But compound mode statistics shows sub-Poissonian statistics. So, photon-phonon antibunching is possible and degree of antibunching factor can be controlled via order number.

Photon-phonon entanglement is also observed in the dynamics of the system, which is verified by both Duan et al and Hillery-Zubairy criteria. Higher order study shows that degree of entanglement increases as order grows. This study may be useful for macroscopic entangled state generation.